Optical properties of thallium films studied with synchrotron radiation

G. Jézéquel and J. Thomas
Laboratoire de Spectroscopie du Solide, Faculté des Sciences de l'Université de Rennes I, F-35042 Rennes Cédex, France and Laboratoire d'Utilisation du Rayonnement Electromagnétique, Université de Paris–Sud, F-91405 Orsay, France

I. Pollini
Dipartimento di Fisica dell'Università di Milano, via Celoria 16, I-20133 Milano, Italy
(Received 3 November 1987)

Near-normal-incidence reflectance (2–11 eV) and multiangle reflectance measurements (11–30 eV) of thallium films evaporated on low-temperature (77 K) Pyrex substrates have been performed in ultrahigh vacuum ($\geq 5\times 10^{-10}$ torr). Optical and dielectric functions have been obtained by Kramers-Kronig analysis and multiangle techniques. The results are discussed in terms of direct interband transitions, both at critical points and between parallel bands, by considering the relativistic augmented-plane-wave (APW) and linear muffin-tin orbital calculations of the band structure of thallium. The optical data, i.e., $\omega^2\epsilon_2$ spectra, are well described as far as 7 eV by the APW calculation with the value $\alpha=\frac{2}{3}$ for the exchange coefficient, if one takes for the peak of the calculated density of states of s-like symmetry the s peak observed in x-ray photoemission experiments. The optical conductivity σ then exhibits sharp edges at 12.4 and 14.7 eV due to the onset of transitions from core spin-orbit-split $5d$ states to the Fermi level. Both the optical-absorption edges and the spin-orbit–splitting energies are found to be in good agreement with x-ray photoemission data.

I. INTRODUCTION

The measurement of the optical properties of metals in the visible and ultraviolet (uv) ranges provides important information concerning their electronic structure. The features displayed in the optical conductivity $\sigma(\omega)$ are, in effect, a manifestation of the singular behavior associated with one-electron bands in the joint density of states, only slightly modified by relaxation effects. In polyvalent metals the optical spectrum can be interpreted in terms of Harrison's[1] and Ashcroft's[2] works on parallel-band absorption, in which a direct connection is found between the optical data and some Fourier coefficients of the pseudopotential. Apart from aluminum,[2] Ashcroft's theory has been applied to explain the behavior of $\sigma(\omega)$ of many polyvalent metals, such as indium,[3,4] white tin,[5,6] and lead.[6,7] The optical properties of lead are still discussed in terms of transitions between parallel bands, but the strong spin-orbit coupling requires a comparison with a complete band structure rather than with the bare pseudopotential coefficients, as is, in general, done for light polyvalent metals. Thallium ($Z=81$) is the heaviest element in group III A and spin-orbit effects must be strong. As for the case of lead,[7] it is expected that the band structure should be known throughout the irreducible part of the Brillouin zone (BZ) in order to interpret the optical spectra, although excitation of electrons between parallel or near-parallel one-electron bands can still constitute a major source of the observed optical absorption.[2] The electronic band structure of thallium (Tl) has been calculated in terms of a local pseudopotential model [orthogonalized-plane-wave (OPW) method],[8] and more recently with linear muffin-tin orbital (LMTO) (Ref. 9) and augmented-plane-wave (APW) methods.[10] Photoelectron studies of metal d bands have also been made in the last decade,[11,12] but the first optical experiments relevant to the band structure of thallium have been performed by Ley *et al.*[12] by means of x-ray photoelectron spectroscopy (XPS). In the case of Tl they observed valence bands extending to 7 eV below the Fermi level E_F, and sharp $5d$ peaks at energy 14.53 ± 0.05 and 12.30 ± 0.05 eV. The valence-band binding energies are 4.90 ± 0.25 eV for the $6s$ band and 0.80 ± 0.12 eV for the $6p$ band. The optical properties of thallium films[13,14] and single crystals[15] have been previously studied under ultrahigh conditions only in the near-infrared and visible regions, up to 5 eV. Thus, it was necessary to extend this work up to 30 eV, in order to study the absorption due to interband transitions between states below and above the Fermi level and also between the core $5d$ states and E_F or higher levels. This paper is part of a more general study of the electronic absorption between the d-core states and empty conduction bands in polyvalent metals, such as gallium, indium, tin, and lead.[16] Furthermore, liquid metals have been the most extensively studied by optical spectroscopy recently. Among them, prominent interest is devoted to polyvalent metals[17,18] because of their low melting temperature and the increasing complexity of the electronic structure with higher atomic number Z, a relevant point being the comparison between results obtained in the liquid and solid phases. Besides the fundamental interest, the experimental knowledge of optical parameters of metals is also of technological interest, since multilayered mirrors, that is, metallic films evaporated onto different substrates in ultrahigh vacuum, are basic components of optical apparatus.[19]

Below 503 K thallium has an hexagonal-close-packed crystal structure, with lattice parameters $a=6.497$ a.u. and $c/a=1.593$ at 5.2 K. Compared with the ideal close-packed structure the thallium lattice is somewhat compressed along the direction of the hexagonal axis c.[20]

II. EXPERIMENT

A Koch-Light 99.999%-pure rod of thallium was evaporated from aluminum oxide crucibles with tantalum heaters on Pyrex substrates maintained at liquid-nitrogen temperature. The evaporation was made on cooled substrates in order to obtain low-scattering films. The film thicknesses (1000–4000 Å) were measured with a quartz monitor calibrated by optical-interference methods and finally verified by means of an interference microscope. During the evaporation the pressure remained lower than 1×10^{-9} torr and then returned to its initial value of less than 5×10^{-10} torr within 1–2 min. Upon exposure to air, thallium oxidates rapidly and heavily, so that particular care must be taken during the preparation of samples. Reflectance measurements were carried out both after the film formation and after the film annealing. The annealing was necessary in order to reduce the structural disorder and to obtain some degree of film epitaxy. Afterwards, the films were recooled and measurements were carried out again at low temperature: this is necessary owing to the low Debye temperature of thallium (78 K). A slight epitaxy is confirmed by comparison with the reflectivity data of Castelijns *et al.* on single crystals.[15] The synchrotron radiation from the Orsay storage ring ACO was used as a light source with a normal-incidence monochromator of 1 Å resolution The apparatus used for the optical measurements has been described elsewhere.[21] Optical constants of Tl in the low-energy range (1–11 eV) have been determined by means of a Kramers-Kronig (KK) analysis of the reflectance data. For the determination of the optical constants in the higher-energy region, oblique-incidence reflectance has been performed and a multiangle method used: the optical constants n and k and, hence, the complex dielectric function $\hat{\epsilon}(E)=\epsilon_1+i\epsilon_2$, have been calculated from 12 to 30 eV. The method is based on the general Fresnel equations $R=R(n,k,\theta,P)$ that connect the reflectance coefficient R to the optical constants (n,k), the angle of incidence θ, and the polarization of light, P. The multiangle method consists of measuring R at various angles of incidence (in the case of Tl, from 30° to 80° at every 5°) at closely spaced wavelength intervals (2 Å), over the wavelength range 400–1100 Å. The experimental results are then treated by means of a computer using a least-squares method. For each wavelength, the optical constants n and k are determined by solving a system of two linear equations of the first degree with two unknowns, which results from the conditions which minimize the average quadratic differences between the experimental reflectance and the calculated reflectance obtained by using trial optical constants. The solution of this system gives the corrections (ν,χ) for the initial optical constants, and the procedure is iterated until the corrections are smaller than a prefixed value.[19] As for the light polarization P, this quantity has been determined at the exit slit of the monochromator in a separate experiment. The ultrahigh-vacuum chamber used for the optical measurements has been rotated around the light beam in order to work with partly polarized light ($P<10\%$) over the spectral region of interest: typically, in our experiments we have worked with a degree of polarization $P=0.06$ at 16 eV and $P\simeq0$ at 30 eV.[19]

III. RESULTS

The reflectance measurements were carried out immediately after film formation and annealing: typical results for quasinormal incidence are reported in Fig. 1(a). We can observe that the film annealing increases its reflectance of about 8%: curves 1 and 2 approach each other at low energy, near 4 eV, and at high energy, over 11 eV. As in the case of white tin,[5] we do not obtain a very high reflectance, which indicates that the interband oscillator strength between 4 and 11 eV is still strong.

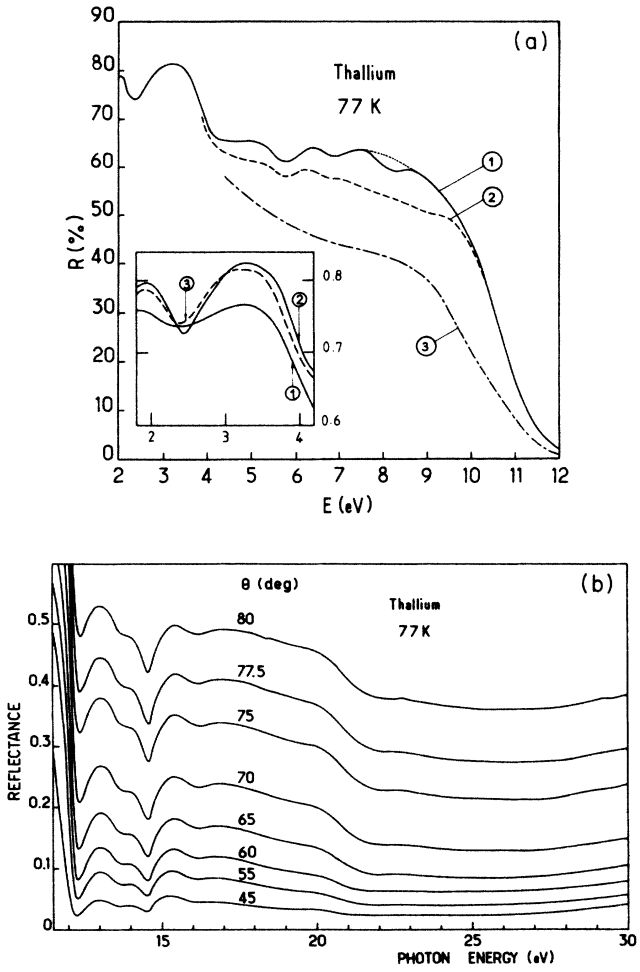

FIG. 1. (a) Reflectance data of thallium films measured at 77 K: (1) annealed films, (2) unannealed films, and (3) evaporated polycrystalline films at 10^{-6} torr (Ref. 14, Arakawa *et al.*). Inset: (1) and (2) Castelijns *et al.* [(1), E⊥c; (2), E∥c]; (3) our data, annealed films. (b) Oblique-incidence reflectance for fixed angles θ of annealed thallium films.

The reflectance drop between 7.6 and 8.8 eV is attributed to a surface-plasmon excitation via the coupling to the film surface roughness. The maximum of the reflectance loss is observed around 8.1 eV, in good agreement with the upper limit for surface-plasmon excitation of 8.3 eV, which can be deduced from the ϵ_1 curve (i.e., for $\mathbf{k}\rightarrow\infty$, $\epsilon_1\rightarrow -1$) (see Fig. 4). We can see in the inset of Fig. 1(a) that between 2 and 4 eV our results are very close to Castelijns's data for E||c, c being the hexagonal axis. This indicates that the film formation presents a certain degree of epitaxy.

In Fig. 1(b) oblique-incidence reflectance results between 11 and 30 eV are shown for fixed values of θ. With the method described in Sec. II, we then determined the optical conductivity $\sigma(\omega)$ shown in Figs. 2 and 3. In the range 0.75–2 eV the curve of $\sigma(\omega)$ is taken from the work of Myers:[13] For polarization perpendicular to the hexagonal axis (E⊥c), a strong peak at 1.35 eV and a shoulder at 1.75 eV (which becomes a peak centered at 1.70 eV for E||c) are observed. Over 2 eV, we can observe a peak at 2.40 eV and a broad, composite band around 4.25 and 4.50 eV (followed by structures around 5.75, 6.95, and 10.25 eV), superimposed on the decaying profile of the σ curve. Such a $1/\omega^2$ dependence was shown by

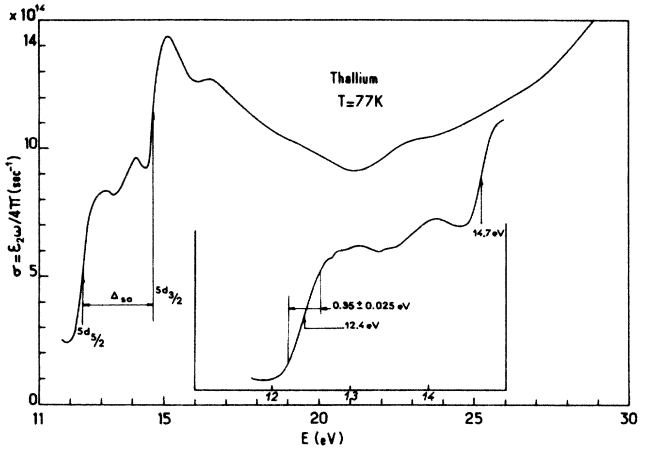

FIG. 3. Optical conductivity of thallium at 77 K in the region of d-core electron excitations to p- and f-symmetry conduction bands.

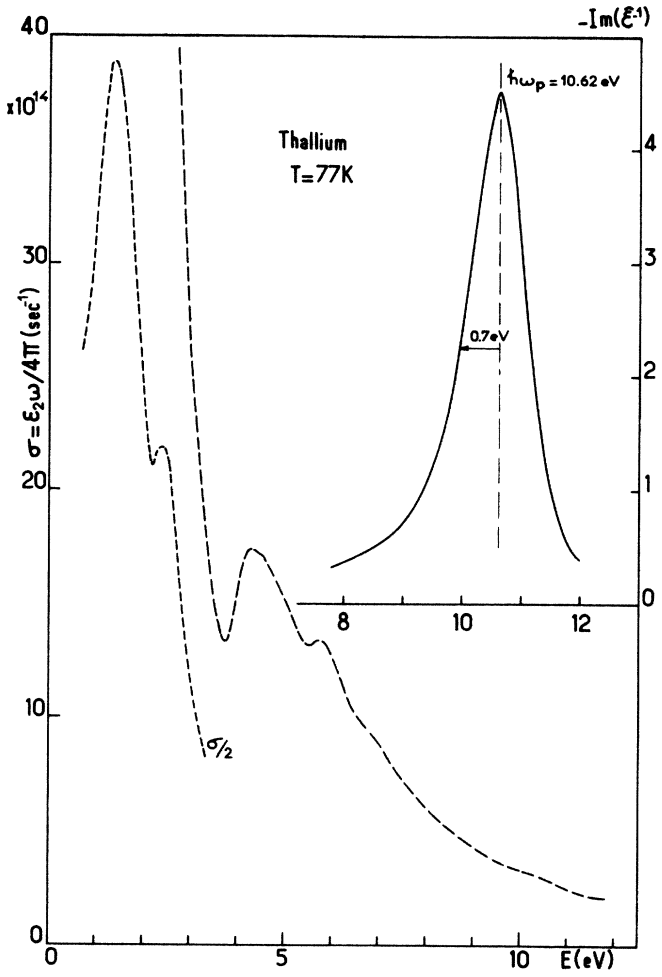

FIG. 2. Optical conductivity of thallium at 77 K in the region of interband transitions and energy-loss function $-\mathrm{Im}\hat{\epsilon}^{-1}$. The plasmon maximum occurring at $\hbar\omega_p = 10.62\pm0.05$ eV is shown. The σ curve below 2 eV has been reproduced by applying the Kramers-Kronig relations to the Myers data (Myers, Ref. 11).

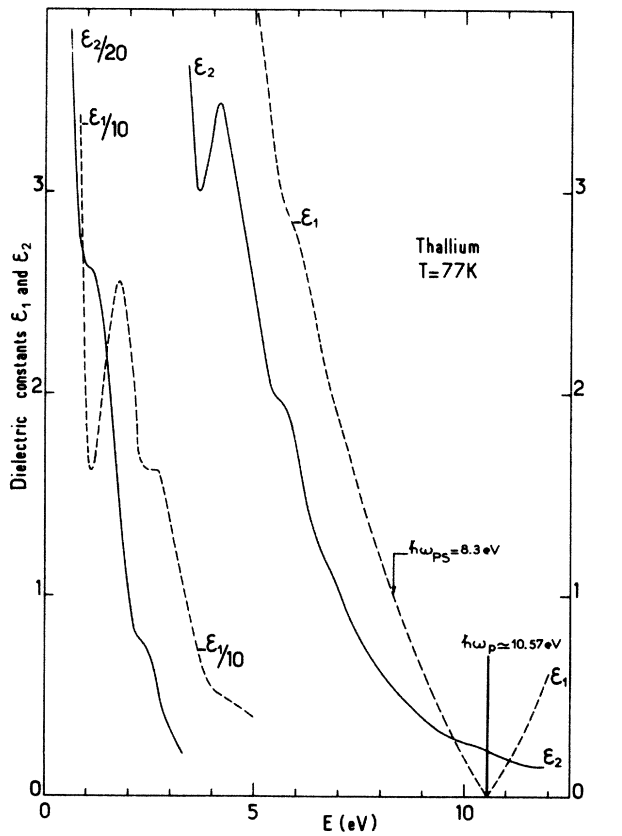

FIG. 4. Dielectric functions ϵ_1 and ϵ_2 of thallium at 77 K. At low energy the Myers data have been used (Ref. 13). The volume plasmon maximum at $\hbar\omega_p = 10.57$ eV and the surface plasmon at $\hbar\omega_{ps} = 8.3$ eV are indicated. ϵ_1 ($\cdots$) and ϵ_2 (——).

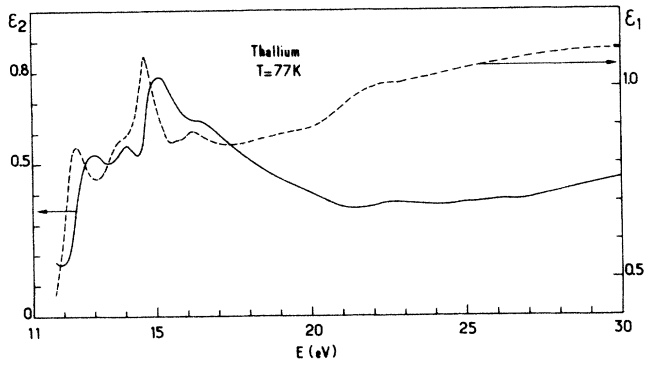

FIG. 5. Dielectric functions ϵ_1 and ϵ_2 of thallium, obtained by means of the multiangle method, as explained in detail in Ref. 19 (Thomas *et al.*).

Cohen[22] to occur in the general case where interband excitation of conduction electrons takes place in a wide energy region. In Fig. 2 the optical energy-loss function $-\mathrm{Im}(\hat{\epsilon}^{-1})$ is also plotted. The maximum is found at 10.62 ± 0.05 eV with a full width at half-height of 1.4 eV. In Fig. 3 the σ curve exhibits two sharp rises at 12.40 and 14.70 eV and strong peaks are observed at 13.15, 14.10, 15.20, and 16.30 eV. Beyond a minimum around 21 eV, one can observe a continuous rise of the optical conductivity as far as 30 eV.

Figures 4 and 5 present the real and imaginary parts of the dielectric function, obtained via the KK relations as far as 11–12 eV and by multiangle reflectance in the remaining range of measurement. In Fig. 4 the energies of the volume and surface plasmons are also reported.

IV. DISCUSSION

We now wish to discuss the optical spectra of thallium in terms of direct interband transitions, due to critical-point and parallel-band absorption. The comparison between electronic band-structure results and spectroscopic data is essential, since in the case of metals it enables us to test the accuracy of theoretical bands several eV above and below the Fermi level. In particular, accurate reflectance and XPS spectra are necessary. It is worth repeating that the presence of parallel bands still provides important information for the description of the optical behavior of thallium, together with analysis of critical-point absorption. The knowledge of partial joint densities of states (JDOS), which have major importance in the energy interval of interest, are very valuable in order to make correct band-transition assignments and to interpret the optical features displayed by the experimental density of states $\omega^2\epsilon_2(\omega)$. We briefly recall, for the sake of clarity, that, where we consider direct interband transitions only, the imaginary part of the complex dielectric function $\hat{\epsilon}(\omega)$ can be written as

$$\omega^2\epsilon_2(\omega)=\sum_{\substack{i,j\\(i<f)}} M_{if}J_{if} ,$$

where J_{if} represents the partial JDOS for bands i and f, where $E_i<E_F<E_f$, and M_{if} is the corresponding transition probability matrix element, which is here assumed to be independent of the wave vector $\mathbf{k}$. The quantity J_{if} is determined by the band structure,

$$J_{if}=\frac{1}{8\pi^3}\int_{\mathrm{BZ}}\delta(E_f(\mathbf{k})-E_i(\mathbf{k})-\hbar\omega)d\mathbf{k} ,$$

and the integral is performed within the irreducible part of the Brillouin zone (BZ).

For the discussion of the optical spectra we shall refer to a recent, relativistic band structure of thallium. In Fig. 6 we report the band structure of Tl along symmetry lines for the exchange parameters $\alpha=\frac{2}{3}$ (solid curve) and $\alpha=1$ (dots), calculated by Ament and de Vroomen (AdV),[10] together with the density of states (DOS) obtained for $\alpha=\frac{2}{3}$. In Fig. 7 the Tl band structure and DOS calculated by Holtham, Jan, and Skriver (HJS),[9] for $\alpha=1$, is also reproduced. Our assignments, based on the reported band structure, together with attributions proposed in the framework of the AdV and HJS calculations,

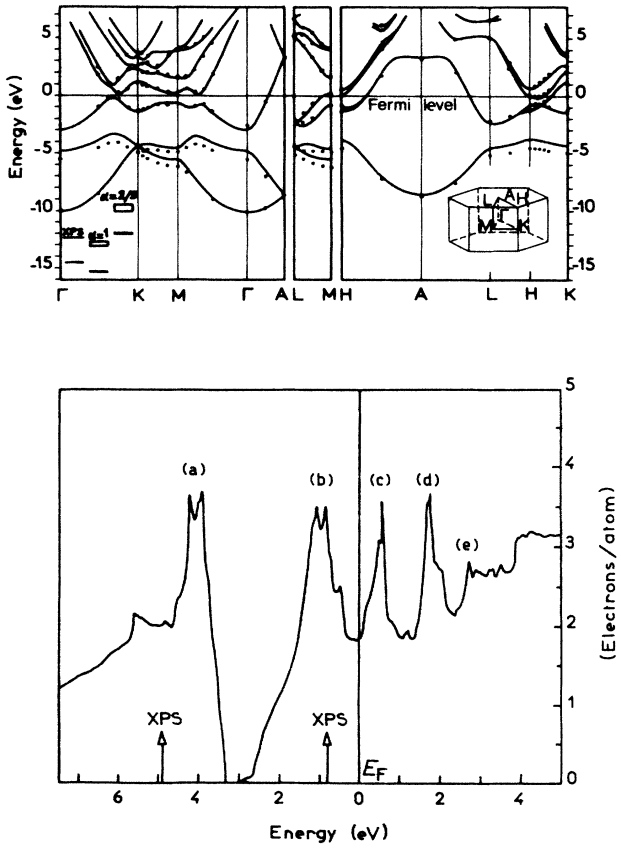

FIG. 6. Band structure of thallium along symmetry lines for exchange parameters $\alpha=\frac{2}{3}$ (solid curve) and $\alpha=1$ (dots) according to AdV (Ref. 10), and density of states.

are summarized in Table I. In the spectrum of the DOS shown in Fig. 6, the XPS peaks observed by Ley *et al.*[12] are also indicated and the DOS peaks related to the electronic bands 2, 3, 4, and 5 are denoted by *A*, *B*, *C*, and *D*, respectively. Peaks *A* and *B* in the valence-band density of states, close to 4 and 1 eV below E_F, present *s*-like and *p*-like character. In particular, the *p*-peak position, which is due to critical points of band 3 (see Table II of Ref. 10), is in good agreement with the XPS 6*p* band, whose valence-band binding energy is 0.80±0.12 eV.[12] The position of this peak is not significantly altered when using the full Slater exchange potential ($\alpha=1$). The peak *s*, which is instead due to critical points of band 4 of *s*-like character (see Table II of Ref. 10, where the critical-point energies are given for a single band with respect to the Fermi energy), shows an energy discrepancy of about 0.9 eV with the XPS 6*s* band observed at 4.90±0.25 eV below E_F.[12] This band, however, can shift 0.6–0.7 eV towards lower energies for $\alpha=1$, thereby showing better agreement with experiment. One also finds that the position of the *d* bands is in much better accordance with the XPS values if $\alpha=1$ is used. Thus, it seems that for the 6*s*-like bands and the deep 5*d* states a stronger exchange potential ($\alpha=1$) would be more appropriate.

In the DOS spectrum of Fig. 7, we find a better agreement between peaks *A* and *B* and XPS peaks: In particular, the energy difference between peak *A* (*s*-like symmetry, band 2) and the corresponding XPS peak is about 0.4 eV.

These points are important for the discussion of the optical spectra and the assignments of the electronic transitions, marked in Fig. 8 by arrows, and listed in Table I. In order to take into account the preceding conclusions deduced from XPS spectra, in Table I we have shifted the *s* band of the calculated band structure by 0.9 eV in the AdV band scheme ($\alpha=\frac{2}{3}$) and by 0.4 eV in the HJS band structure ($\alpha=1$).

We can at once remark that the comparison between optical data and band structure confirms that bands 3 and 4 (taken in order of increasing energy) are the best calculated in both cases. This is also in accordance with the fact that a description of the third and fourth zone surfaces are virtually insensitive to the different values of α employed in calculations. In fact, the optical assignments are easily made by considering 3→4 transitions and the peaks of the partial JDOS, J_{34}, reported in Refs. 9 and 10 and in Table I. For example, the peak at 1.56 eV due to J_{34} in the HJS calculation corresponds to the average of the peaks observed at 1.35 and 1.75 eV for E⊥c.[15] We assign the following peak at 2.50 eV to

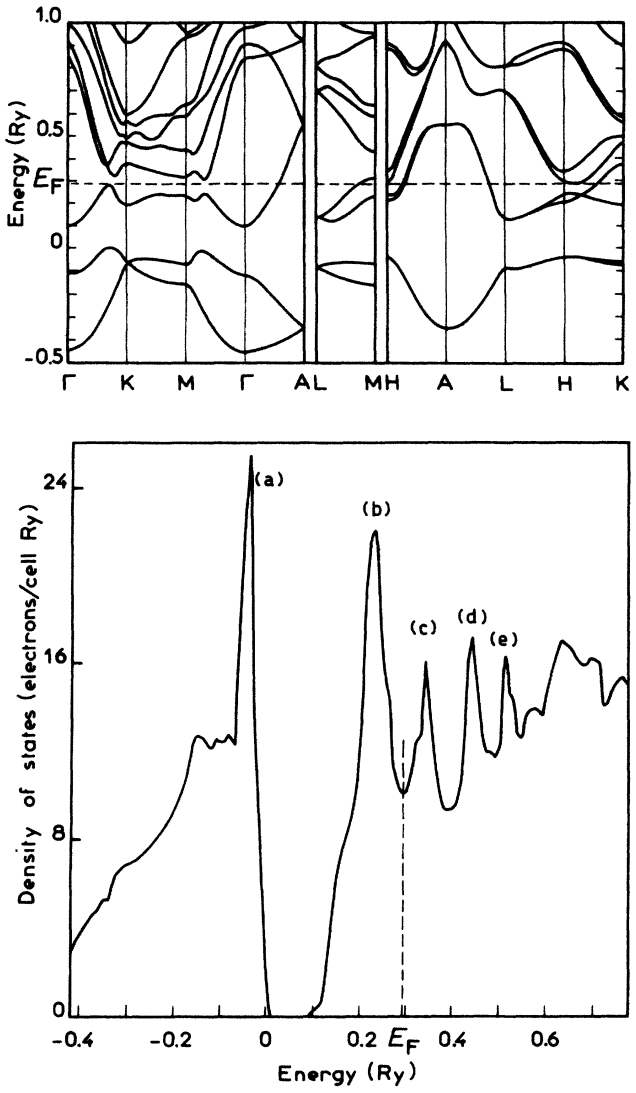

FIG. 7. Fully relativistic energy-band structure of thallium along the symmetry directions ΓKMΓ, *LM*, and *HALHK* according to HJS (Ref. 9). Two energy scales (Ry and eV) are shown in order to compare the theoretical bands with experimental data (eV). The density of states is also shown.

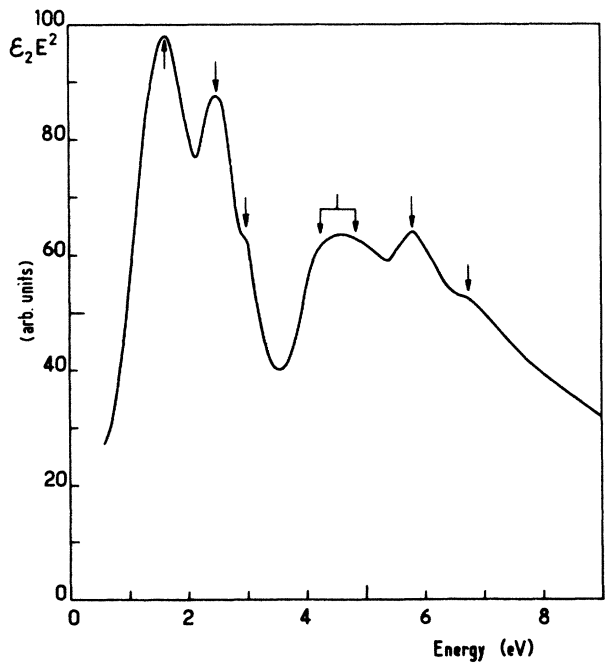

FIG. 8. Optical joint density of states ($\epsilon_2\omega^2$) for thallium between 1 and 9 eV.

parallel-band absorption, $3\rightarrow5$: By considering the critical-point absorption J_{35}, according to HJS an energy difference of 0.35 eV with respect to the experimental peak is found. This difference is, however, reduced to 0.1 eV in the AdV band scheme, by considering critical-point absorption. Thus, for band 5, the comparison of $\omega^2\epsilon_2(\omega)$ spectra with the theoretical JDOS suggests that this band should be lowered by about 0.35 eV in the calculations HJS ($\alpha=1$) and only by 0.10 eV in those of AdV ($\alpha=\frac{2}{3}$). It is interesting to note that for the fifth zone surface a band shift of 200 meV in the vicinity of E_F is proposed in the work[9] of HJS, in order to account for the dumbbell dimensions and to reach better agreement with the AdV calculation. It also appears that this band shift is related to the different values of α, as shown by the better agreement of the HJS and AdV calculations with $\alpha=1$ of band 5. The structure centered at 4.60 eV, due to critical-point absorption J_{36} according to HJS, shows a discrepancy of 0.7 eV for band 6, since the JDOS peak is at 3.9 eV. In the AdV scheme we find instead better agreement for this peak, by considering critical-point absorption. We have also attributed this peak to $2\rightarrow4$ critical-point transitions in view of the good agreement: In this case an energy scaling of 0.3 eV between calculated and experimental transitions would be necessary. The peak at 5.85 eV is due to parallel-band absorption and is assigned to $2\rightarrow4$ transitions along the $K-M$ line. Also, critical-point absorption for transitions $2\rightarrow5$ along the symmetry line $\Gamma-M$ should be considered. In the HJS scheme, the compensating shift of 0.4 eV due to the shifts of band 2 towards greater binding energies and of band 5 towards the Fermi level also allow one to assign the optical peak to $2\rightarrow5$ transitions. Finally, the structure at 6.80–7 eV assigned to parallel-band absorption $1\rightarrow4$ and $2\rightarrow5$ along the symmetry line $K-M$ is well accounted for either by considering a shift of 0.9 eV for band 2 or the two downward shifts of 0.4 eV for bands 2 and 5. In the AdV scheme a difference of 250 meV between the optical spectra and band scheme still remains.

Caution should be used when employing the DOS spectra for the interpretation of the optical peaks. In effect, we find that the energy differences found in the DOS peaks correspond well to the observed peaks in optical spectra and also to the direct interband transitions listed in Table I. This agreement between DOS and optical energies is often possible, since the critical points responsible for the DOS peaks are found in the band schemes at the same $\mathbf{k}$ values below and above E_F.

From the foregoing discussion we can conclude that the accurate determination of the $\omega^2\epsilon_2(\omega)$ spectra allows one to find some differences between the band schemes in which the Slater value ($\alpha=1$) or the Gaspar-Kohn-Sham value ($\alpha=\frac{2}{3}$) for the exchange coefficient is used. In effect, we think that although it is not completely satis-

TABLE I. Our optical data are compared with the peaks of Myers (Ref. 13) and Castelijns *et al.* (Ref. 15) in columns 1 and 2. In column 3 our assignments, based on critical point (CP) and parallel-band absorption are made within the framework of the APW (Ament–de Vroomen, Ref. 10) and LMTO (Holtham-Jan-Skriver, Ref. 9) band structures. Both joint density of states (JDOS) and density of states (DOS) peaks are also considered for the interpretation of optical structures. The exchange parameters $\alpha=\frac{2}{3}$ and 1 are used in the AdV and HJS band calculations, respectively. All energies are in eV.

$\epsilon_2\omega^2$ Experiment			Theory			
		Our	Ament and de Vroomen[c]		Holtham-Jan-Skriver[d]	
This work	Other work	assignments	CP	JDOS	CP	JDOS
1.65	1.35 **E**⊥**c**[a] 1.75 1.70 **E**∥**c**[a] 1.40[b]	$3\rightarrow4$	1.4 ΓMK plane 1.63 ΓM line	1.35 **E**⊥**c** 1.95 1.55 **E**∥**c**	large regions in Brillouin zone	1.55
2.50	2.55[a] 2.45[b]	$3\rightarrow5$ close to $K-M$ line	2.65 (ΓMK) 2.85 ($HKML$)	2.55		2.85
3.0	3.0[b]	$3\rightarrow5$ CP close to K point ($K-M$)				
4.6	4.4 **E**∥**c**[a]	$2\rightarrow4$ CP near M ($\Gamma-M$) CP near K ($\Gamma-K$)	4.5 4.65	4.9	4.65 5.00	
5.85		$2\rightarrow4$ along $K-M$ $2\rightarrow5$ CP ($\Gamma-M$ line) close to M	5.85 6.3	5.5 (DOS) 6.3	5.90 6.35	
6.80		$1\rightarrow4$ along $K-M$ $2\rightarrow5$ along $K-M$	6.8 7.15	6.7 (DOS)	6.90 7.30	6.9 (DOS)

[a]Castelijns *et al.* (Ref. 15).
[b]Myers (Ref. 11).
[c]Band structure for $\alpha=\frac{2}{3}$; s bands (1 and 2) shifted downwards by 0.9 eV.
[d]Band structure for $\alpha=1$; s bands (1 and 2) shifted downwards by 0.4 eV.

factory, the AdV band structure with $\alpha=\frac{2}{3}$ better describes the optical properties as far as 7 eV, provided the energy peak for the density of states of s symmetry is shifted towards the XPS s peak, or, in other words, where a shift of 0.9 eV for the s peak is allowed. In these cases, a complete agreement for the optical structures at 5.85 and 6.80 eV is reached.

In conclusion, we have found some correlation between the position of the electronic bands of thallium and the exchange parameter α. In particular, it appears that the exchange-interaction influence on the optical spectra is small or negligible, where one considers electronic states near E_F, and can become considerable for higher excited states (bands 5 and 6) or lower full states (bands 1 and 2).

Optical transitions from core d states to E_F still have to be discussed. We remind the reader that thallium is a polyvalent metal belonging to group III with three valence electrons: $6s^2$ and $6p$. The next-lowest states are the $5d^{10}$ levels, approximately 12 eV below E_F, which for all practical purposes can be considered flat: d-state excitations to the Fermi level ($5d_{5/2}\rightarrow E_F$ at 12.40 eV and $5d_{3/2}\rightarrow E_F$ at 14.70 eV) give rise to two sharp edges in the σ curve which originate from the spin-orbit splitting of the $5d$ levels. The optical determination of the d-core binding energies (at 12.40 and 14.70 eV) for the states $5d_{5/2}$ and $5d_{3/2}$ gives values very close to the XPS values (at 12.30 and 14.53 eV, respectively) measured by Ley *et al.*[12] By considering the accuracy of the Fermi-level positioning in XPS spectra, we can conclude that the XPS and optical determination of d-core binding energies are in very good agreement. The only remaining contribution to the σ curve at higher energies is observed as a structureless, continuous rise of the absorption beyond 20 eV, assigned to $5d^{10}\rightarrow 6f$ band transitions. This transition gives, in fact, a strong, broad band which possibly extends as far as 60–100 eV, and of which we only observe the rising edge. In Fig. 9 we compare the experimental conductivity observed between the edges $5d_{5/2}$ and $5d_{3/2}$ to the calculated DOS obtained by AdV and HJS. The Fermi energy E_F has been adjusted to the $d_{5/2}$ edge. The DOS curves show two sharp peaks in this range: the first at 0.7 eV beyond E_F and the second at 1.8 eV beyond E_F. This second edge is, in the AdV calculation, 2 eV higher than in the calculation of HJS. These two peaks are well defined in the experimental spectra, although they are broadened by lifetime effects (the d edges are well represented by a convolution of the Fermi level in the DOS curves with reference to the vacuum level by means of Lorentzian curves with a half-width of about 0.4 eV). Their peak positions are in fine agreement with the assignments made: the first structure due to the critical regions of band 4 is well assigned in both band schemes, while the second structure, assigned to the critical region of band 5. is only displaced by 0.1 eV in the AdV band structure and by 0.3 eV in the HJS scheme.

V. CONCLUSIONS

The optical spectra of high-quality films of thallium can be interpreted in terms of relativistic band-structure

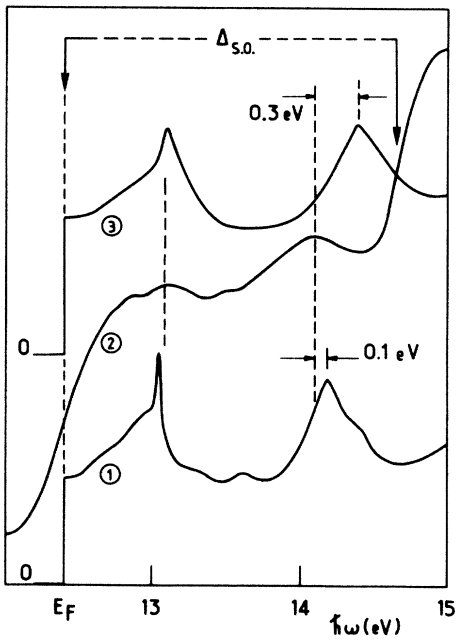

FIG. 9. Conductivity of thallium between the $d_{5/2}$ and $d_{3/2}$ edges [curve (2)] compared to the density of empty states according to Ament and de Vroomen [curve (1)] and Holham *et al.* [curve (3)].

diagrams, by taking, for the exchange parameter of the Slater free-electron equation,

$$V_{X\alpha}(\mathbf{r})=-6\alpha[3\rho(\mathbf{r})/8\pi]^{1/3}\ ,$$

[$\rho(\mathbf{r})$ is the electron density] either the Slater value ($\alpha=1$) or the Gaspar-Kohn-Sham value ($\alpha=\frac{2}{3}$) in order to make a critical comparison between experimental quantities and the calculated results, obtained by Ament–de Vroomen (APW) and Holtham-Jan-Skriver (LMTO). This interpretation can be improved if the value of α is empirically adjusted so as to better approximate a realistic exchange-correlation potential. In fact, discrepancies between calculations and optical data are only to be ascribed to a lack of self-consistency of the crystal charge density and to a neglect of correlation effects, namely, to the rough approximation made for the exchange interaction. This is not surprising since the exchange-correlation potential should be nonlocal (in effect, it should be $\mathbf{k}$ dependent) and, besides, should depend on the energies of the electronic state. In this sense, better agreement with experiment should be reached, if one makes use of the exchange-correlation potential introduced by Hedin and Lundqvist[23] (HL). In the case of lead, for instance, the comparison between the photoemission data[24] and the energy-band calculations[25] obtained by a fully relativistic approximation, employing the HL potential, shows an agreement of better than 0.1 eV for full states.

We still note that the optical data of Tl allow one to obtain a general spectrum of the density of states, located between the Fermi level and the ionization energy E_b. Integrated density of states (bremsstrahlung isochromat

spectroscopy) and angle-resolved inverse photoemission would then allow one to get more detailed spectra of the empty states or the density of excited states.

ACKNOWLEDGMENTS

The authors thank the technical staff of the linear accelerator of the storage ring ACO of the Université de Paris–Sud for providing the light beam during the experimental runs. The manuscript was written while one of them (I.P.) was visiting the University of Rennes I. It is a pleasure for him to acknowledge the kind hospitality enjoyed at the "Laboratoire de Spectroscopie du Solide," which is "Unité Associé au Centre Nationale de la Recherche Scientifique (CNRS) No. 1202." The Laboratoire d'Utilisation du Rayonnement Electromagnetique is "Laboratoire propre du CNRS conventioné à l'Université Paris–Sud." The Dipartimento di Fisica dell'Università di Milano is affiliated with the Gruppo Nazionale di Struttura della Materia del Consiglio Nazionale delle Ricerche.

[1]W. A. Harrison, Phys. Rev. **147**, 467 (1966).
[2]M. W. Ashcroft and K. Stürm, Phys. Rev. B **3**, 1898 (1971).
[3]A. G. Mathewson and H. P. Myers, J. Phys. C **5**, 2503 (1972).
[4]J. C. Lemonnier, G. Jézéquel, and J. Thomas, J. Phys. C **8**, 2812 (1975).
[5]G. Jézéquel, J. C. Lemonnier, and J. Thomas, J. Phys. F **7**, 2613 (1977).
[6]G. Jézéquel, J. Thomas, and J. C. Lemonnier, Solid State Commun. **23**, 559 (1977).
[7]J. C. Lemonnier, M. Priol, and S. Robin, Phys. Rev. B **8**, 5452 (1973).
[8]P. M. Holtham and M. G. Priestley, J. Phys. F **1**, 621 (1971).
[9]P. M. Holtham, J. P. Jan, and H. L. Skriver, J. Phys. F **7**, 635 (1977).
[10]M. A. E. A. Ament and A. R. de Vroomen, J. Phys. F **7**, 97 (1977).
[11]R. T. Poole, P. C. Kemeny, J. Liesegang, J. C. Jenkin, and R. C. G. Leckey, J. Phys. F **3**, L 46 (1973).
[12]L. Ley, R. Pollak, S. Kowalczyk, and D. A. Shirley, Phys. Lett. **41A**, 429 (1972).
[13]H. P. Myers, J. Phys. F **3**, 1078 (1973).
[14]E. T. Arakawa, R. N. Hamm, W. F. Hauson, and T. P. Jelinek, in *Optical Properties and Electronic Structure of Metals and Alloys*, edited by F. Abelès (North-Holland, Amsterdam, 1966), p. 384.
[15]J. H. P. Castelijns, J. P. C. P. Derks, and A. R. de Vroomen, J. Phys. F **5**, 2407 (1975).
[16]G. Jézéquel, J. Thomas, and I. Pollini (unpublished).
[17]P. Oelhafen, G. Indlekofer, and H. J. Güntherodt, in Proceedings of the 6th International Conference on Liquid and Amorphous Metals, Garmisch-Partenkirchen, 1986 (unpublished).
[18]T. Inagaki, E. T. Arakawa, A. R. Cathers, and K. A. Glastad, Phys. Rev. B **25**, 6130 (1982).
[19]J. Thomas, G. Jézéquel, and I. Pollini, J. Opt. Soc. Am. A (to be published).
[20]C. S. Barrett, Phys. Rev. **110**, 1071 (1958).
[21]J. C. Lemonnier, J. Thomas, and S. Robin, J. Phys. E **6**, 553 (1973).
[22]M. H. Cohen, Philos. Mag. **3**, 762 (1958).
[23]L. Hedin and B. I. Lundqvist, J. Phys. C **4**, 2066 (1971).
[24]G. Jézéquel, thèse d'Etat, Université de Rennes I, 1984, p. 194.
[25]K. Horn, B. Reihl, A. Zartner, D. E. Eastman, K. Herman, and J. Noffke, Phys. Rev. B **30**, 1711 (1984).